Computational and Structural Biotechnology Journal 27 (2025) 1648–1659

Contents lists available at ScienceDirect

Computational and Structural Biotechnology Journal

journal homepage: www.elsevier.com/locate/csbj

Research Article

Three scenarios for amyloid transformation in the context of the funnel model

I. Roterman [a,*], M. Słupina [b], D. Dułak [c], L. Konieczny [d]

[a] Department of Bioinformatics and Telemedicine, Jagiellonian University Medical College, ul. Medyczna 7, Kraków 30-688, Poland
[b] ALSTOM ZWUS Sp. z o.o., Modelarska 12, Katowice 40-142, Poland
[c] ASSA ABLOY Opening Solutions, Magazynowa 4, Leszno, Poland
[d] Chair of Medical Biochemistry, Jagiellonian University Medical College, ul. Kopernika 7, Kraków 31-034, Poland

ARTICLE INFO

Keywords:
Amyloids
Transthyretin
α-synuclein
VL domain of IgG
Tau
AlphaFold
Funnel model

ABSTRACT

Analysis of the structure of proteins based on the evaluation of their geometric structure (secondary and supersecondary structure) can be extended to assess the structuring of the hydrophobic region of a protein. Such analysis of amyloid protein structures leads to the identification of three scenarios for amyloid formation. One is the loss of the micelle-like ordering present in the native form (a centric hydrophobic nucleus with a polar surface) in favour of a disordered distribution of hydrophobicity in the amyloid form. The term "micelle-like" is to be understood as specific hydrophobic burial. The second scenario is the reverse process, when the highly disordered distribution of hydrophobicity in the native form is replaced by a hydrophobic burial after amyloid transformation. These two scenarios have been identified for pathological (neurodegenerative) amyloids. The third scenario is the presence of hydrophobic burial ordering in a functional amyloid fibril. In this case, this ordering is present both in the fibril and in the single chain that is the building block of the fibril. This hydrophobic burial ordering provides a means of self-control of fibril size. It prevents unrestricted fibril propagation, which in the case of pathological amyloids is the main factor that disrupts the normal functioning of organelles in the amyloid surroundings. Population analysis (including numerous polymorphic forms) was performed using a collection of structures deposited in the Amyloid Atlas database. These observations allow the construction of a kind of amyloid funnel model, in which the energy minimum depends on external, environmental conditions that may be evaluated using the fuzzy oil drop model in its modified version (FOD-M).

1. Introduction

The well-known phenomenon of protein complex formation is based on specific targeting by defining the site of complexation. For example, these include complexes using surfaces exhibiting hydrophobic exposure for the interface or building together a structure representing a micelle-like system treated as specific hydrophobic collapse [1]. However, the orientation of the complexation process can be altered by external factors such as salt concentration (ionic strength), pH or the presence of organic molecules [2]. In the context of properly constructed complexes, the phenomenon of generating amyloid structures is marked by certain distinctive features. These include the predominant presence of the β-structure form enabling the formation of interchain hydrogen bond networks on long-chain fragments, but also sometimes along the entire chain length. The predominance of β-structure also results in a 2D (flat) form, as opposed to the spatial (3D) structure commonly found in proteins and protein complexes. The term 2D is related to the backbone orientation of a single chain in the fibril. The side chains are oriented (according to sp^2 carbon-hydrogen hybridisation) out of plane, which introduces an element of spatiality, although it does not apply to the backbone.

Micelle and micelle-like – terms used in this paper – are understood as the construction with a centric hydrophobicity concentration with a gradually increased level of hydrophobicity reaching the zero level on the surface. The zero level of hydrophobicity means the polar surface. The scale of hydrophobicity is transformed to the range (1−0). The presence of a centric hydrophobic core with a polar surface is also expressed in this paper as hydrophobic burial or hydrophobic collapse.

A review of amyloid structures, including in their polymorphic forms, is possible thanks to the availability of a database called Amyloid

* Corresponding author.
E-mail addresses: myroterm@cyf-kr.edu.pl (I. Roterman), mateusz.slupina@wp.pl (M. Słupina), mbkoniec@cyf-kr.edu.pl (L. Konieczny).

https://doi.org/10.1016/j.csbj.2025.04.016
Received 21 February 2025; Received in revised form 9 April 2025; Accepted 10 April 2025
Available online 13 April 2025

Atlas [3,4]. It has also been shown that almost any protein can form amyloid forms, which is mainly achieved by shaking [5]. It is a mystery how this form is obtained *in vivo*, where it is difficult to identify an analogous factor. Pathological amyloids are characterised by significant stability and resistance to proteolysis. They do not undergo chemical denaturation (even under the influence of detergents) [6]. In the process of amyloid transformation (similarly to other protein folding processes) intermediate structures are identified [7]. It is expected that identification of the intermediates' properties can be used in designing therapies for early amyloid transformation. The structures experimentally obtained using laboratory techniques (shaking under strictly defined environmental conditions), show structuring identical to the forms identified in human brains; however, this is limited to the tau amyloid [8–10].

The model, fuzzy oil drop (FOD-M), applied to the analysis of amyloid structures assumed the micellisation process as the mechanism for the specific structuralisation of proteins. The amino acids are treated as the set of different bipolar molecules, which, limited by covalent bonds in the polypeptide chain, are able to generate only the micelle-like structures. The term micelle-like expresses the tendency to concentrate the hydrophobic residues in the central part, with the exposure of polar residues on the surface [11]. The highly symmetrical organisation of the hydrophobic burial is not possible due to the limited mobility of amino acids restricted by the peptide bonds in the polypeptide chain. The degree of post-hydrophobic-collapse ordering is reached by different proteins in differing degrees. However, the proteins representing the highly symmetrical order of hydrophobic burial organisation are identified (downhill, fast-folding, ultrafast-folding [12]). Additionally, a large majority of domains treated as individual structural units represent ordering accordant with hydrophobic core with polar surface organisation. The main argument to treat the proteins as having micelle-like organisation is supported by the water environment, which is the critical condition for any organism. The polar environment as delivered by water is the source of the assumed organisation of bipolar molecules in the form of micelles.

Polar water is not the only environment in which the proteins are active. The membrane representing the opposite form of the surrounding – the hydrophobic one – is assumed also to direct the folding process of proteins anchored in the membrane. The introduction of the FOD-M model taking into account the environment in the form of the external force field for the folding process is expressed as the function of the continuous form. The 3D Gaussian function is assumed to be the effect of the polar water's directional role in the folding process; however, the other environments present in the cell, like the membrane, endoplasmic reticulum and Golgi apparatus, as well as chaperones and chaperonins (also including prefoldin) deliver different external force fields for the folding process. The FOD-M model is able to characterise the protein's structures as the effect of water and other environmental factors' participation in the folding process in a quantitative form.

The criterion used in this paper to classify the amyloid forms available in [3,4] is based on an assessment of the hydrophobicity distribution of both the native form (if available) and the amyloid form. The native form and status of the single chain (fibril component), amyloid fibril (protofilament) and superfibril status are evaluated. Term "superfibril" is used to express the structural form constructed by more than one protofilament.

The distribution of hydrophobicity is important because of the possibility of determining the environmental conditions under which the process of protein folding as well as amyloid transformation occur. The particular distinguishing feature of the single chain structures – fibril components – is expressed in 2D form, as opposed to biologically active proteins with a 3D form. It is assumed that the preference for the 2D form is related to the properties of the air/water interphase, the presence of which increases significantly during shaking. In this phenomenon, environmental specificity with the significant presence of air/water interphase is critical to the generation of 2D forms. Therefore, the use of a model that quantifies the environment's contribution to shaping the structure seems justified.

The main goal of the presented analysis is the interpretation of the structural transformation of native proteins into their amyloid forms, including pathological as well as functional examples. The proposal of the revised form of the funnel model introducing the mathematical dependency on the search for the local/global energy minimum is presented.

2. Materials and methods

2.1. Data

The proteins discussed in detail in the current paper are listed in Table 1. and Table 2. The analysis included native forms as well as the corresponding amyloid forms for comparison purposes. In addition to pathological amyloid proteins, the list also includes endorphin, which shows its biological activity in the form of an amyloid fibril.

In addition, all amyloids included in Amyloid Atlas [3,4] representing the amyloid groups listed in Table 1 were analysed. However, their description is limited to an aggregate analysis.

All amyloids available in Amyloid Atlas representing the VL domain of IgG, transthyretin, α-synuclein, A-Beta and TAU amyloids are under consideration. The detailed analysis is presented for selected examples. The selection of examples was to perform comparable analysis with the proteins discussed in other papers. The selection of two examples of α-synuclein was to explain the source of the vast difference between the status of this protein in those structural forms of amyloids.

The calculation and analysis of others (not presented in detail in this paper) are available using the very simple tools available in an open access system (see Materials and Methods – Programs used). As is shown later on in this paper, the differences in the structures of amyloid forms for certain proteins are rather low, which suggests the similarity of their interpretation. The main aim is to visualise three scenarios for amyloid formation in the discussed examples. These three scenarios can be visualised in the form of the funnel model for amyloid formation taking the native structural forms of the discussed proteins.

2.2. Description of the FOD-M model used

The principles of the fuzzy oil drop (FOD) model and its modified version (FOD-M) have already been described in numerous papers [28,29]. Here, the basics are cited for ease of results interpretation.

The model is based on the assumption that, in an aqueous environment, bipolar molecules (which is what all 20 amino acids are) tend to structure themselves towards an organisation with a centrally located hydrophobic core with a polar surface. This arrangement ensures solubility in an aqueous environment, where the vast majority of proteins show their activity. The distribution of hydrophobicity in an idealised micelle is described by a 3D Gaussian function spanning the body of the protein:

Table 1
List of proteins analysed in detail in this paper.

NAME	PDB ID	FORM	REF
VL domain of IgG light chain	4BJL	native	[13]
VL domain of IgG light chain	6HUD	amyloid	[14]
Transthyretin	1DVQ	native	[15]
Transthyretin	6SDZ	amyloid	[16]
α-synuclein	1XQ8	native	[17]
α-synuclein	2N0A	amyloid	[18]
α-synuclein	6XYO	amyloid	[19]
TAU	5O3L	amyloid	[20]
Endorphin	6TUB	amyloid/native – hormone	[21]

Table 2
Amyloids in terms of their role in the organism. Percentages for VL domain – frequency of deposits localisation in diseases.

Amyloid	Role in organism – disease
VL domain of IgG	Heart – 75 %, kidney – 65 % [22]
Transthyretin	nerves, ligaments, heart, and arterioles, and systemic amyloidosis, hereditary ATTR (ATTRv) [23]
α-synuclein	Parkinson's, Alzheimer's, Lewy bodies, multiple system atrophy [24]
TAU	Parkinson's disease, dementia with Lewy bodies and multiple system atrophy [25]
Endorphin	Parkinson's, Alzheimer's [26]
	Physiological – hormone [27]

$$T_i = \frac{1}{\sum_{i=1}^{N} T_i} \exp\left[\frac{-(x_i-\bar{x})^2}{2\sigma_x^2}\right] \exp\left[\frac{-(y_i-\bar{y})^2}{2\sigma_y^2}\right] \exp\left[\frac{-(z_i-\bar{z})^2}{2\sigma_z^2}\right] \quad (1)$$

Where x_i, y_i and z_i represent the positions of the effective atoms (the averaged position of the atoms comprising a given *i-th* amino acid). The parameters σ_x, σ_y and σ_z are the parameters of the Gaussian function. The common orientation is defined to calculate the appropriate values for the σ_x, σ_y and σ_z parameters. The two positions of the atoms of the greatest distance define the orientation along the x-axis. The greatest distance between the projections on the YZ plane defines the orientation along the y-axis.

The positions of the most distant positions of the effector atoms take on a 3σ value in each direction (according to the three-sigma rule). The 3D Gaussian function spanning the protein body expresses the size and shape of a given molecule depending on the relationship of the σ_x, σ_y and σ_z parameter values. The values $\sigma_x = \sigma_y = \sigma_z$ indicate a sphere. The T_i value indicates the level of hydrophobicity in an idealised distribution consistent with the micelle-like system assigned to the *i-th* amino acid in question. T_i is assumed to represent the theoretical, idealised level of hydrophobicity represented by the effective *i-th* atom in its spatial position in the protein body encapsulated in the ellipsoid (3D Gaussian function).

However, the levels of hydrophobicity in a given protein can be and usually are different with respect to the idealised form. The level of observed hydrophobicity (O_i) is the result of an inter-residue interaction, which is determined by a function proposed by M. Levitt [30]:

$$O_i = \frac{1}{\sum_{i=1}^{N} O_i} \sum_{i=1}^{N} \begin{cases} \left(H_i^r + H_j^r\right)\left(1 - \frac{1}{2}\left(7\left(\frac{r_{ij}}{c}\right)^2 - 9\left(\frac{r_{ij}}{c}\right)^4 + 5\left(\frac{r_{ij}}{c}\right)^6 - \left(\frac{r_{ij}}{c}\right)^8\right)\right), for r_{ij} \le c \\ 0, for r_{ij} > c \end{cases} \quad (2)$$

Where c is the cutoff distance. A c= 9 Å was adopted (after M. Levitt [30]). H^r stands for the intrinsic hydrophobicity assigned to each amino acid (any hydrophobicity scale can be adopted [31]).

A comparison of the T and O distributions can be made after prior normalisation of both distributions (sum of all $T_i = 1$ and sum of all $O_i = 1$). Normalisation is expressed in Eq. 1 and Eq. 2 by the first terms in both equations.

Comparing the T distribution with the O distribution provides information on the extent to which the hydrophobic collapse system has been opened up in a given structure. An aqueous environment favours the generation of this type of system. Any deviation to the hydrophobic burial system analysed provides information about the specific nature of the structure in question, but also about the conditions under which the folding process occurs.

Comparison and quantitative evaluation of differences is carried out using the divergence entropy proposed by Kullback-Leibler [32]:

$$D_{KL}(O|T) = \sum_{i=1}^{N} O_i \log_2 \frac{O_i}{T_i} \quad (3)$$

However, the D_{KL} value is not interpretable (entropy). Therefore, a second reference R distribution was introduced, in which $R_i = 1/N$ where N is the number of amino acids in the chain. R distribution means assigning each amino acid (effective atom) an equal level of hydrophobicity. It is a distribution without a hydrophobic core and any differentiation in the status of individual amino acids.

Comparison of the $D_{KL}(O|T)$ and $D_{KL}(O|R)$ values allows the similarity of the O distribution to the T and R distributions to be assessed. The relation $D_{KL}(O|T) < D_{KL}(O|R)$ is interpreted as the presence of a hydrophobic core in the protein body. In order to avoid using two values to describe the same object (the protein being analysed), a measure of RD (relative distance) was introduced:

$$RD = \frac{D_{KL}(O|T)}{D_{KL}(O|T) + D_{KL}(O|R)} \quad (4)$$

The RD value is in the range (0−1). The RD< 0.5 value is interpreted as the presence of a hydrophobic core. However, the structure of the hydrophobic core can vary, which is precisely what the RD value expresses. The closer the value is to 0, the more pronounced the hydrophobic core is in a given protein. An RD close to 1 indicates an approximation to a uniform distribution of hydrophobicity without marked variation within a given protein.

The RD value can be determined for any defined structural unit: domain, chain or complex. For each of the listed units, a 3D Gaussian function is constructed to suit the size and shape of the unit. The interpretation of the results (RD values) then relates to the status of the selected structural unit.

With the proposed method, it is also possible to determine the status of the selected part of the structure (chain in a complex, domain in a chain, or any selected part of a chain). In this case, the O_i, T_i and R_i values representing the selected fragment are normalised. Calculation of the D_{KL} and RD values for the selected fragment is performed according to the procedure given. The RD value thus obtained allows an assessment of the contribution of the selected fragment to the hydrophobic core construction within the structural unit from which the fragment was taken. It can participate in the construction of the core but can also be a part of the structure that introduces local incompatibility.

The aqueous environment directing the protein structuring process (protein folding) towards a hydrophobic-collapse-based structure is not the only environment for protein activity. A membrane is the opposite environment to polar water conditions, requiring the exposure of hydrophobic residues on the surface and often (especially in the case of an ion channel) the location of polar residues in the central part of the protein. This is the opposite arrangement to the one previously discussed. This means that a 1–3D Gaussian function should be used to describe such a distribution. In practice, the T_{MAX}-T_i function is used, where T_{MAX} is the maximum value in a given T distribution. However, it turns out that the hydrophobicity distribution in a membrane protein applies to the function:

$$Mi = Ti + [K * [T_{MAX} - Ti]_n]_n \quad (5)$$

Where K is a parameter that modifies the 3D Gaussian function. The

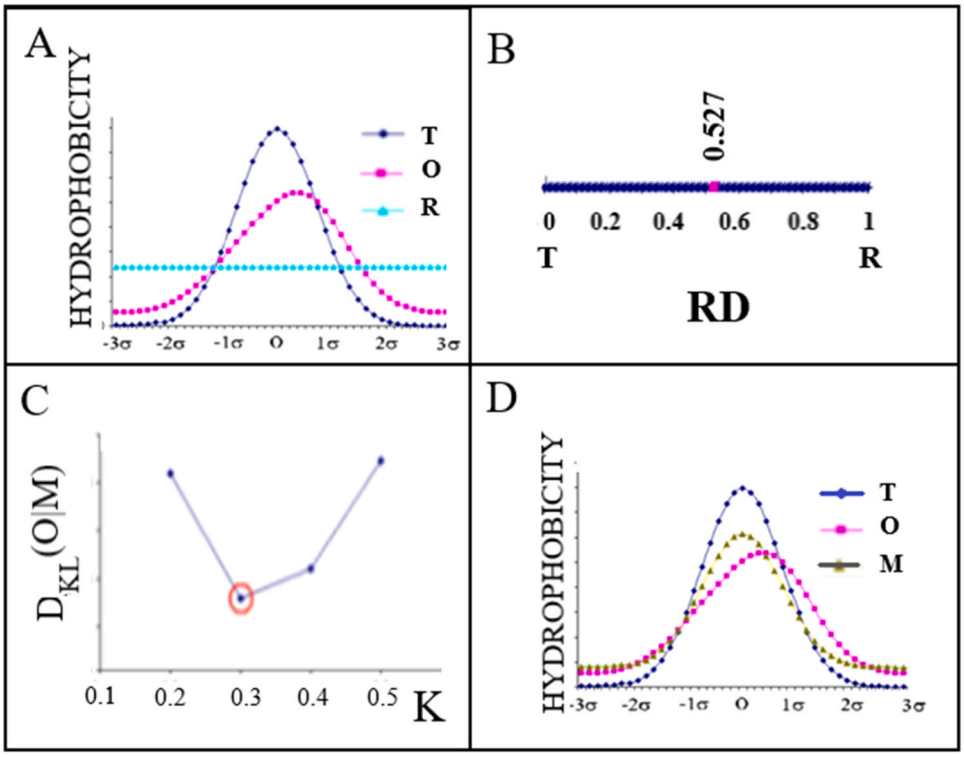

Fig. 1. Graphical presentation of the model used (reduced to 1D). A – T, O and R profiles, B – determined value RD = 0.527 for this example, indicating distribution a little bit above the threshold, C – determination of the optimum value of K through iterative search, D – T, O and M distributions for a designated value K = 0.3, indicating significant contribution of the aqueous environment to shaping of the structure.

degree of this modification is expressed precisely by the value of this parameter. The higher it is, the stronger the contribution of the "inverted" distribution and the more it deviates from a system with a centric core and polar surface. The value of the K parameter is determined iteratively to obtain the minimum value of $D_{KL}(O|M)$.

A graphical representation of the model in question is given in Fig. 1. The hypothetical example of the Gaussian type and the observed one is generated in the one-dimensional presentation to explain the methodology of the FOD-M model (Fig. 1A). The Gaussian function (blue in Fig. 1A) is compared with the observed distribution (pink inn Fig. 1A). According to the FOD-M model, the R distribution of equal level of hydrophobicity is calculated and visualised as a turquoise line. The dots on each position in these distributions visualise the levels of the appropriate hydrophobicity level. The scale expressed by the σ parameter is to show the Gaussian character of the T distribution. The x-axis in the described protein examples (below in this paper) expressed the sequence of amino acids in the appropriate chain. The positions of T_i, O_i and R_i expressed the level of hydrophobicity attributed to the particular effective atom. The application of Eq. 3 and Eq. 4 produces the RD value that is shown on the spectrum of the whole range for this parameter. RD values are limited to the range (0−1) according to the definition (Eq. 4). The value of RD calculated for the discussed example is equal to 0.527, which is shown in Fig. 1B.

To search for the theoretical distribution expressed by Eq. 5, the iterative calculation is performed with values of K changed. The set of different Mi distribution is calculated to find the lowest value of $D_{KL}(O|M)$ (Fig. 1C). It is shown in the discussed example that modification of T distribution by K= 0.3 delivers the best approach of T distribution to O distribution. It suggests that the hypothetical "folding chain" status that is shown in Fig. 1A was following the external conditions expressed by Mi with K= 0.3. The M distribution – the most appropriate for the O distribution – is shown in Fig. 1D (grey line). It means that the hypothetical "protein" in this case followed the external condition modified in respect of the polar water external conditions. The protein folded in the polar water conditions represents the structure with the O distribution following the T distribution with K= 0.0. This is not the case in this discussed example.

The interpretation of the M distribution is as follows: Assuming that the protein folds to adapt to external conditions in a polar water environment (K=0.0), hydrophobic residues become concentrated in the central part with simultaneous exposure of polar residues on the surface. In altered environmental conditions, the folding protein also adapts to the surrounding environment by adopting an ordering that is consistent with the specifics of that environment. Therefore, it is assumed that the determined function M denotes the external force field for the folding process.

An overview of the many protein structures showing adaptation to varying conditions is given in numerous papers written by the team (including, for example, [28]).

The model discussed was applied in the present work to interpret amyloid protein structuring. The native and amyloid structures of the proteins were analysed, with both structural forms available. The structural unit is: single chain, protofilament and superfibril (if present for the amyloid in question). Superfibril is used here to identify the forms constructed by more than one protofilament.

The term "status" is used quite often in this paper. It expresses the hydrophobicity distribution as observed and interpreted in each discussed protein. Status may be of a high hydrophobic burial form with a hydrophobic core and polar surface, or the distribution described by higher K values, which means the form of disorganisation of a typical hydrophobic core construction (fuzzy hydrophobic centre with differentiated surface).

2.3. *Programs used*

The VMD program was used for 3D presentations of the proteins' structures [33,34].

The program enabling calculation of *RD* is accessible on the GitHub

platform: https://github.com/KatarzynaStapor/FODmodel and on the https://hphob.sano.science platform.

3. Results

All the proteins analysed here in their *in vivo* and amyloid forms are characterised by means of profiles visualising the hydrophobicity distribution:

A – theoretical, T – consistent with the distribution expressed by means of a 3D Gaussian function spread over the protein body.

B – observed, O – expressing the actual state of a given amino acid resulting from inter-residue hydrophobic interactions.

C – the comparison of these two distributions is expressed by the value RD, which indicates the proximity of the O distribution to the reference T distribution. RD< 0.5 means a structure with a present, centric hydrophobic nucleus and a polar shell.

D – the environmental influence on the structure of a given protein, amyloid fibril I of a single chain – a fibril component. A value K< 0.5 is interpreted as a structure orientated towards a water environment. Any higher value of this parameter is interpreted as the influence of external factors (external force field).

E – M – distribution of hydrophobicity modified by the folding environment. M distribution means the distribution that is optimal in a given environment. This distribution is described by the K value as the form of the distribution depends on the K value.

3.1. Amyloids with a known native structure

The environment-influenced structural changes can be observed in amyloid transformation not requiring any mutation. The classification of proteins whose WT structures and amyloid form are known suggests a proposal for defining the mechanism of amyloid transformation. Examples of proteins are transthyretin [15,16], α-synuclein [17–20], the VL domain of IgG light chain [13,14] and endorphin representing physiologically active amyloids [21] (Table 3).

Table 3 provides RD and K parameter values for the native forms and for their amyloid forms. In the case of amyloids formed by VL domain of IgG and transthyretin, a change in structuring characteristics is evident, involving a significant increase in the values of these parameters as a result of amyloid transformation. This means that the native functional form represents a status similar to a hydrophobic core with polar surface system. These are proteins that operate in an aqueous environment. Hence, adaptation to the requirements of this environment is present. Amyloid transformation – which, as evidenced by experiments, requires significant environmental changes – is expressed here by a significant increase in the values of the RD and K parameters.

Table 3
Parameters describing the native and amyloid forms. The fibril and single chain status is described for endorphin. The domains: D1 and D2 within the structure of amyloid 6XYO-A define the pseudo domains distinguished in the structure of this protofilament. The chain fragments forming pseudo domains are given in the "Fragment" column. The provision of chain segment ranges for VL domain and transthyretin is due to the composition of the amyloid form of these proteins.

NATIVE				AMYLOID			
PDB ID	Fragment	RD	K	K	RD	Fragment	PDB ID
TRANSTHYRETIN							
1DVQ	10–120	0.580	0.5				
	11–35	0.616	0.6	1.7	0.717	11–35	6SDZ
	57–123					57–123	
V_L of IgG							
4BJL	1–110	0.555	0.5				
	1–37	0.461	0.3	1.2	0.773	1–37	6HUD
	66–105					66–105	
α-SYNUCLEIN							
1XQ8	1–140	0.643	1.3	0.3	0.472	1–140	2N0A
				0.4	0.531	30–100	2N0A
				1.2	0.720	14–94	6XYO-A
				0.0	0.294	14–34	6XYO-A-D1
				0.3	0.473	44–94	6XYO-A-D2
				0.4	0.526	21–99	6XYO-B
				1.7	0.711		6XYO-AB
ENDORPHIN							
6TUB	CHAIN	0.493	0.3	0.2	0.385	FIBRIL	6TUB

A different characteristic is represented by α-synuclein, which in its native form occurs in a system with a "permanent chaperone" in the form of axon terminals of presynaptic neurons. The structure available in PDB presents the α-synuclein in complex with micelle, which is assumed to mimic the target molecules for this protein in its native form [17]. The very high K value for this protein suggests the structure greatly contrasts with the regular hydrophobic core with polar surface arrangement (in respect of the standard folding system with a hydrophobic core and polar surface at least in part). Such a high K value suggests the necessary presence of a "supporting molecule" to keep this unusual structure for the chain. Hence the observed high RD and K values for the native form resulting from the imposed structural form guaranteeing complexation to the neuron. An α-synuclein amyloid identified in an aqueous environment adapts its structuring to these very conditions [18]. Low RD and K values for the amyloid form indicate this type of amyloid transformation (Fig. 2 and Fig. 3). The superfibril form present in PDB ID 6XYO reveals regular hydrophobic core with polar surface structuring in one protofibril, while the other protofilament (the superfibril component) shows high RD and K values (Fig. 2, Fig. 3).

The unique protofilament status (chains A, C, E, G, I) of α-synuclein (in relation to the other forms of polymorphic α-synuclein), expressed by the high value of the K parameter indicating a regular hydrophobic core with polar surface arrangement, is due to the two-domain structure of this protofilament: D1 (14−34) and D2 (44−94) (Table 3). The introduction of the pseudo domain division clarifies the mechanism of origin of this protofibril. The status of the domains is indicated in Table 3. It is described by a set of values that are surprisingly low. A visualisation of the interpretation by pseudo domain is provided by Fig. 4.

A similar situation in the form of high RD and K values is shown by the structure of an α-synuclein amyloid (8PK4) [35].

In the structure of the chains of this amyloid, one can distinguish a pseudo domain (60−96) with a status defined by very low RD and K values. The identification of hydrophobic collapse ordering in the pseudo domain systems confirms a mechanism that prefers to generate the fibril structure (including superfibrils) of α-synuclein. This observation confirms the uniqueness of α-synuclein as a protein undergoing amyloid transformation according to a mechanism that seeks to generate a structure based on a hydrophobic burial arrangement.

Of note in Table 3 is the status of the amyloid form of endorphin. The available structure in PDB contains five chains. The status of this arrangement is described by very low RD and K values. This means that the fibril exhibits a hydrophobic core with polar surface arrangement in aqueous environments and therefore a form that functions well in aqueous environments. Furthermore, the status of the single chain also shows an ordering of this type. This means that the form of amyloid available in PDB adapts well to the aqueous environment. Furthermore, it has been shown that such an endorphin fibril status has an up to eight-chain system [36]. A fibril with a higher number of chains is described by progressively higher RD and K values (as the fibril swells). This suggests that the functional endorphin fibril adapts well to the conditions of the aqueous environment. In contrast, the construction of a long fibril would require a change of environment similarly to other amyloids, including those obtained under laboratory conditions [37–40].

3.2. Large scale analysis – polymorphism of amyloid forms

To supplement the results given above, the resources of the amyloid protein database Amyloid Atlas [3,4] were used.

The structural forms available there have been analysed using the

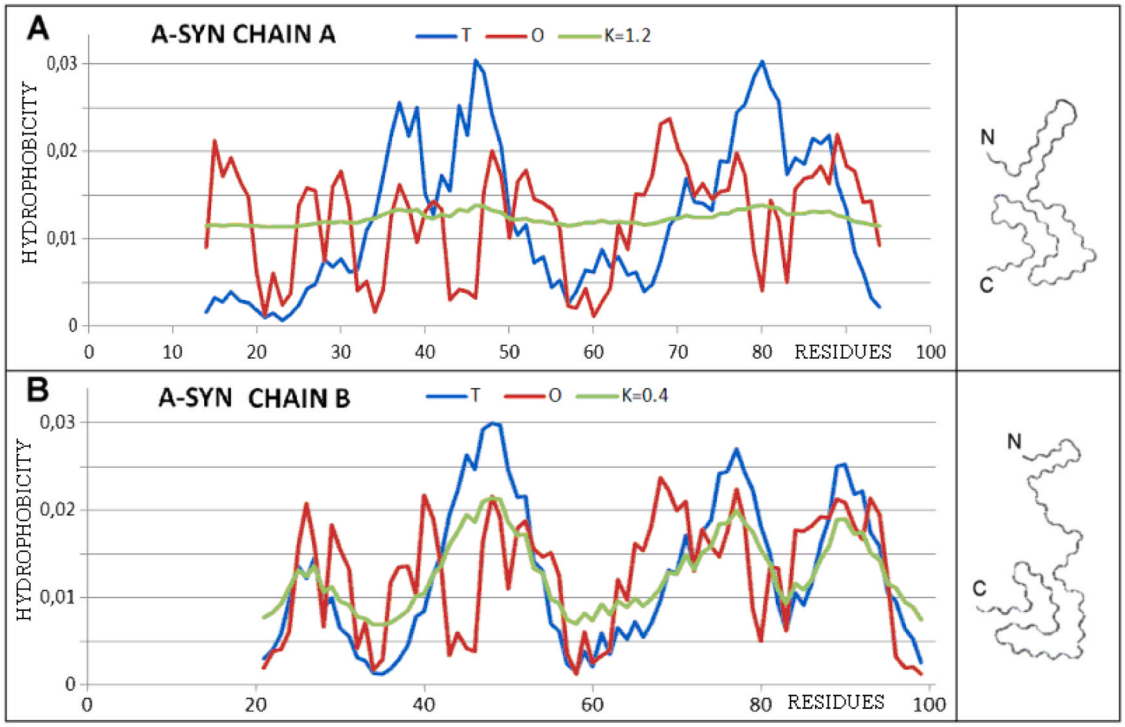

Fig. 2. T (blue), O (red) and M (green) profiles for the K value given in the legend for 6XYO. The amyloid structure for this form of α-synuclein is in the form of a superfibril. The protofilaments are shown here, represented by chains A and B respectively. A – protofilament A, B – protofilament B, 3D presentations of each of the forms discussed are also given respectively.

FOD-M model discussed here.

Of note, Table 4 shows the RD and K values obtained for individual protofibrils, single chains and superfibrils. These results give the status of the structural unit that each of these is. This means that a 3D Gaussian function was generated for each structural unit.

Some of the structures discussed (as reported in the Amyloid Atlas database) are derived from post-mortem material, some are obtained under specific laboratory conditions (e.g. in the presence of ligands or ions, or e.g. heparin). Characteristics are given for the relevant subgroups.

A summary of the results for VL domain of IgG as well as transthyretin shows similar status for fibril and single chain. A very low variation in the results obtained is also evident (Fig. 5A, B).

In the case of A-Beta amyloids, the status of amyloids obtained post-mortem shows no differentiation in terms of the whole group of these amyloids.

In the collection of amyloid structures, tau was distinguished in the Amyloid Atlas database's late and middle intermediates. The middle intermediate status is characterised by the closest approximation to the hydrophobic burial form among all tau amyloid categories. Late intermediate, on the other hand, represents a status close to the averaged form of the entire set of examples.

The forms distinguished and discussed in [7,8] as PHFs (paired helical filaments) show no dissimilarity to the entire group of examples discussed.

Characterisation of α-synuclein shows populationally low values of both RD and K compared to the other amyloid examples discussed here. Due to this specificity, groups were distinguished according to the range of values of the K parameter. The majority (56 %) show a status expressed by a K value of < 0.5. This observation is a notable exception to the other examples of amyloids discussed here. The structure of the post-mortem-derived α-synuclein amyloid group is characterised by a low range of RD and K values.

The reported change in RD and K parameter values for single amyloid structures and WT form for VL and transthyretin are confirmed in the population analysis. Fig. 5 visualises the relationship between the determined values of the K parameter for the different ranges of this parameter. In both cases, a significant increase in K parameter values after amyloid transformation is evident. In the light of the FOD-M model, this implies the need for a significant change in environmental conditions of a nature different to that created by water.

A different form of α-synuclein amyloid transformation is visualised in Fig. 5C, where the direction of change is reversed compared to VL domain and transthyretin.

Characterisation of the A-Beta amyloid forms shows low values for the K parameter, which can be interpreted as representation of near hydrophobic collapse structures by amyloids of this group. However, the range and variation of K parameter values is quite dispersed (Fig. 6).

Alternative structures of α-synuclein [41], chains with A-Beta sequences obtained using a program that directs structuring towards the generation of hydrophobic core with polar surface forms have been shown to be very diverse and dubious [42,43], as have models obtained using I-TASSER [44–47] and Robetta [48,49]. The listed programs provided a whole spectrum of structures with varying statuses expressed in RD values from hydrophobic collapse forms to structures with RD above 0.8. All of these models represented single chain structures, the form of which did not allow for the possibility of fibrils. This subject, however, requires in-depth analysis [50].

All the amyloids discussed appear to represent polymorphic forms as is also shown for tau amyloids (Fig. 7). This is probably due to the different sources of the samples, especially of patients-delivery representing specific disease differentiation.

4. Discussion

The formation of amyloid fibrils *in vitro* confirms a strong influence of environmental conditions [51,52]. The description of the polymorphic forms discussed in this paper indicates a dependence of the structure on the external force field. Experiments also show the need for partial unfolding of the native structure [6,7,43]. A potential *in silico*

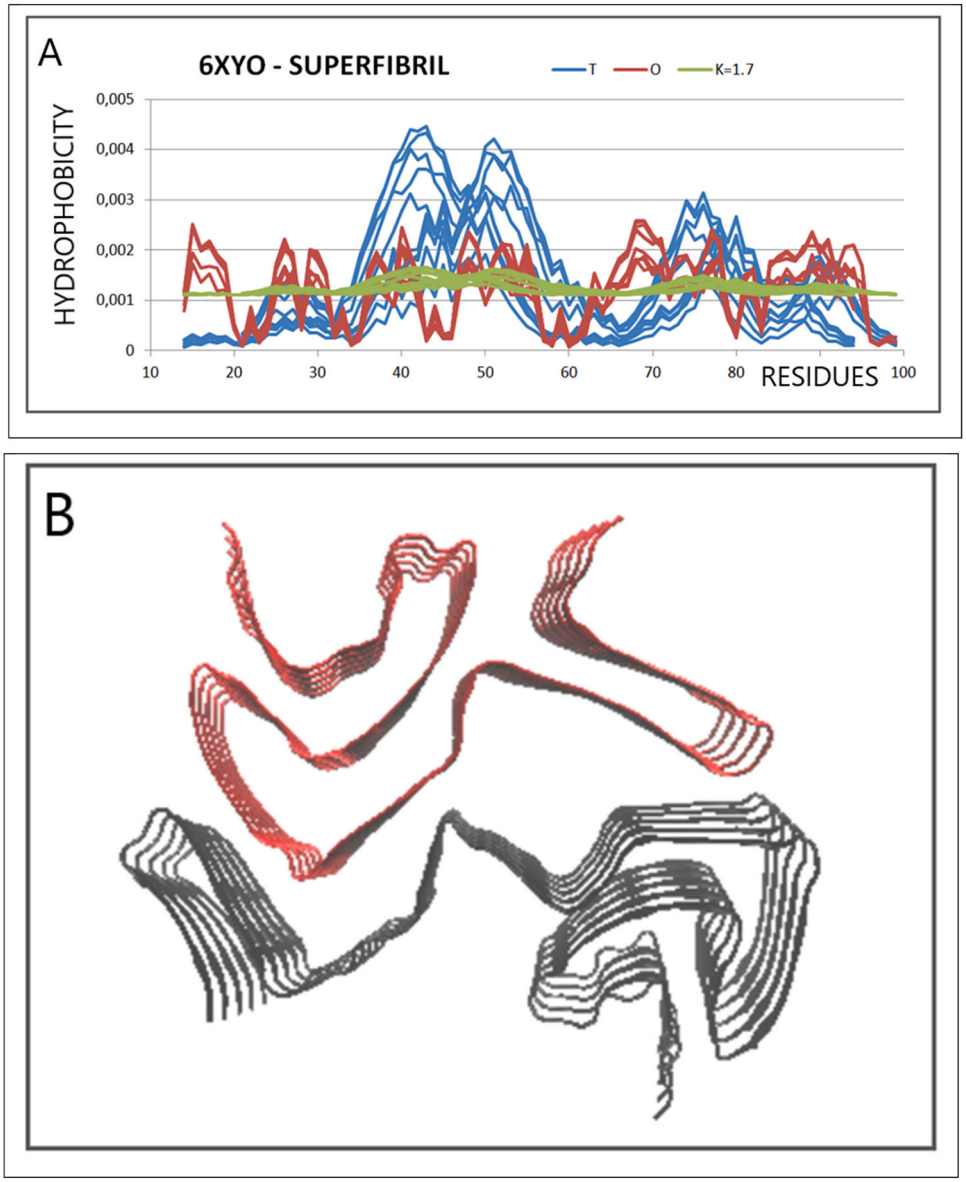

Fig. 3. Structure 6XYO – superfibril A – summary of profiles T, O and M for K= 1.7 B – 3D structure of superfibril – protofilament chain A – black, protofilament chain B – red.

simulation of the amyloid transformation process starting from the native form should take into account partial unfolding. In contrast, the folding process leading to the amyloid form should take place in the presence of an external force field expressed as an M Eq. 5.

Maintaining a procedure for optimising internal impacts should also be taken into account. As a result, the *in silico* optimisation procedure leading to the amyloid structure should be regarded as multiple-object optimisation [53]. The target function determining the amyloid structure is the result of an optimisation taking into account both the internal force field (non-bonding interaction between atoms in protein) and the external force field (conditions imposed by the environment – adjustment of the hydrophobicity distribution to the external field form). The proposed function takes the following form:

$$F(r_{ij}) = F[E_{INT}(r_{ij}) + E_{EXT}(K, r_{ij})] \quad (6)$$

The E_{INT} function expresses non-binding interactions between atoms present in the protein structure (internal force field). This function depends on the variables that are the distances between the interacting atoms – r_{ij}.

The E_{EXT} function – also depending on r_{ij} – expresses the active involvement of the environment in the amyloid transformation process. It is important to note the significant role played by the K parameter in this function. It can be treated as an independent variable and subject to change in the search for the optimal solution. Another form of simulation is to carry out an optimisation of the E_{EXT} function at a given fixed value of the K parameter.

The functions E_{INT} and E_{EXT} are intentionally called E due to the main role of energy in the force field definition.

The solution to the problem of multiple-object optimisation is the technique called Pareto front [54]. This procedure is planned to be applied to simulate the amyloid transformation of proteins.

Polymorphic forms of amyloids as dependent on external force field conditions – which is expressed by the value of K – may be presented in form of a funnel model (Fig. 8). Many structural forms are possible depending on the established external conditions directing the process of structural transformation adjusting to the externally imposed force field. The location of the appropriate energy minimum turns out to be dependent on external conditions. A quantitative assessment of this

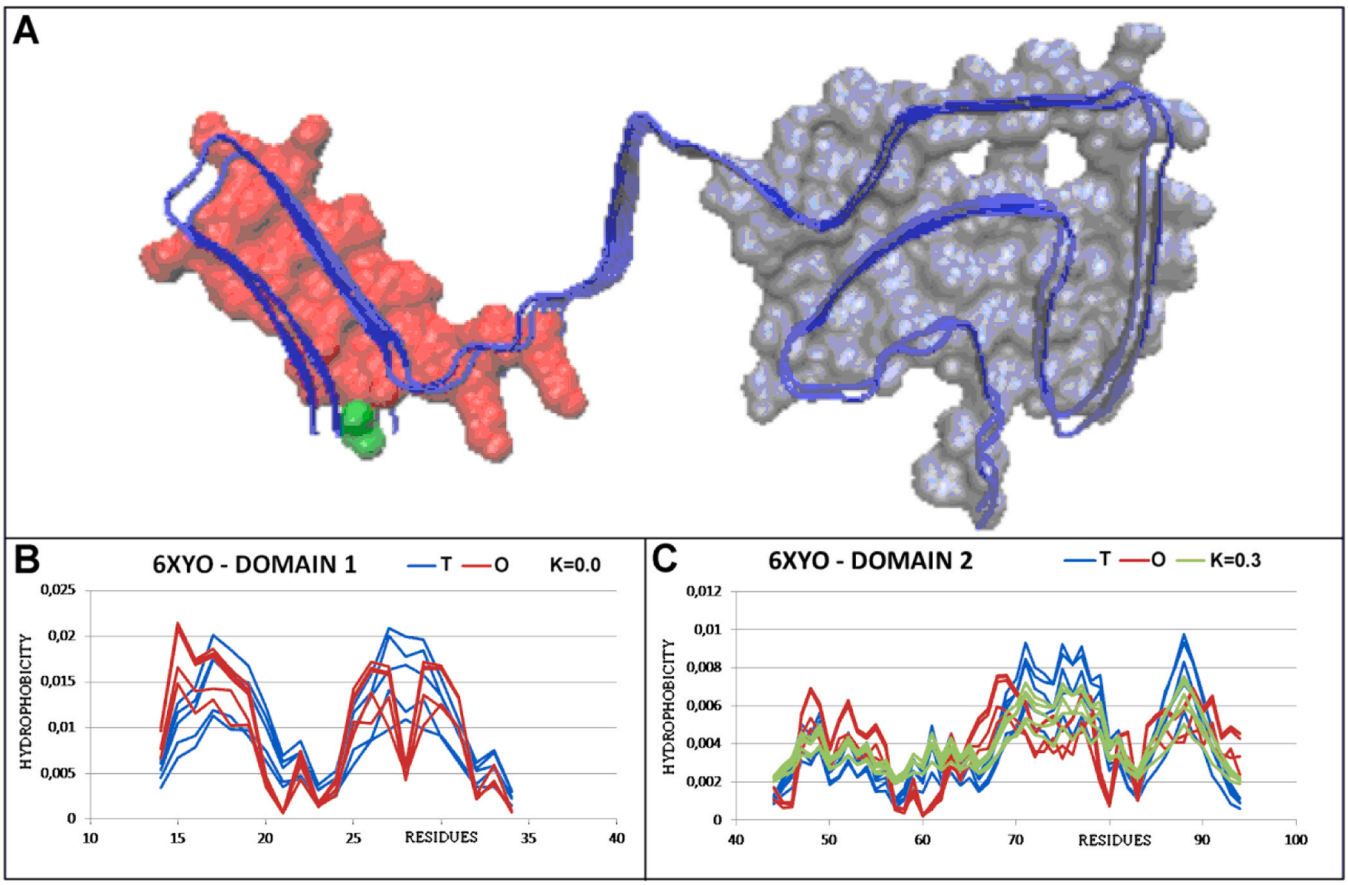

Fig. 4. Protofilament structure (A, C, E, G, I) with pseudo domain division (PDB ID 6XYO): A – 3D presentation: D1 14–34 (red) and D2 44–94 (ice blue) indicate the presence of two hydrophobic cores with polar surface systems. Residue – green – N-terminal residue.B – T and O profiles for part of protofilament A (fragment 14–34) – the M profile is not shown since it is identical to T distribution (K=0.0).C – T, O and M profiles for K= 0.3 for the domain within protofilament A (fragment 44–94).

relationship is illustrated in Fig. 8.

A visualisation of the funnel model for amyloid transformation, Fig. 8 highlights the multiple locations of the energy minimum for the amyloids under discussion. Many local minima for amyloid forms visualise the dependency on the external force field of structuralisation of the amyloid under consideration. The transition from native to amyloid form is characterised by different external conditions distinguishing three scenarios: increase of K value for VL domain and transthyretin, lowering of K value for α-synuclein and constant K value for endorphin, which represent low K value for individual chain as well as for fibril status.

This is a form of expression of polymorphism observed in experiments. A funnel model introducing a scale of values of the K parameter on the horizontal axis provides a proposal for the selection of the path of the folding process as dependent on environmental conditions. The native structures are represented by a well-defined position of the energy minimum, while amyloid forms obtained under different conditions show variation as a result.

A special place in the diagram (Fig. 8) is occupied by endorphin, which in both single-chain and fibril form (here 5 chains) shows structuring consistent with the hydrophobic core surrounded by polar surface. Here, the respective value of the K parameter is constant and dependent on *in vivo* conditions. There are no polymorphic forms expected for endorphin. Polymorphic endorphin structures were obtained through *in vivo* experiments. Factors that have influenced the acquisition of structures different from the native ones are related to the environment (pH, ionic strength). The existence of different structural forms under experimental conditions is possible. However, as it fulfils a hormone role that is critical for the functioning of the body, such variability would be dangerous. The storage and release of hormones must be controlled. The self-preventing mechanism of uncontrolled fibril propagation by limiting its size to a strictly defined number of chains in a fibril was discussed in [36]. Tracking changes in the K value for an elongated fibril (1–24 chains in fibril) reveals a high degree of fibril structure adjustment for 1–8 chains in the fibril. The fibril status of this size shows an exceptionally low order value of $K = 0.2$. As the number of chains in the fibril increases, the K value increases rapidly. This means that the environment enables the formation of fibrils with up to 8 chains. Increasing the number of chains would require environmental support (increasing the value of the K parameter), which does not happen in natural *in vivo* conditions. Therefore, the term was used that polymorphic forms are rather not acceptable under *in vivo* conditions. Of course, it cannot be ruled out that this system could malfunction.

Verification of the proposed model of dependence of the folding process on environmental conditions could be based on an experiment analogous to the folding/unfolding/refolding of fast-folding, ultra-fast-folding proteins in a dialysis bag with the concentration of urea changing in the environment. Instead of urea, alcohol or any other chemical compound can be used. The variability of the concentration and the type of alcohol could easily shed light on the type and degree of contribution of the introduced factor to the folding effect. It seems that this could be a way to find a factor that could turn out to be analogous to those factors that are found under *in vivo* conditions or could potentially appear there.

Verification of the proposed model for the interpretation of structural transformation with regard to endorphin could take the form of lengthening the fibril size of this hormone, provided that the environment changes towards increasing K values.

Table 4
Values in the top row – mean values of RD and K parameters for the structures of the respective amyloids (as available in the Amyloid Atlas database [3,4]). The number of example structures is given under the name of the protein. Columns: fibril, chain, superfibril – upper line – mean value, lower line – standard deviation to express the amount of variation in results. All VL and transthyretin structures were derived from post-mortem analyses. Others were described under distinguishing specific experimental conditions (as reported by the Amyloid Atlas database). PHF – paired helical filament. The percentage values in the left column are the quantitative relationship between different sources of material for structure determination.

AMYLOID	FIBRIL		CHAIN		SUPERFIBRIL	
	RD	K	RD	K	RD	K
TRANSTHYRETIN	0.741	1.71	0.752	1.73		
12	0.02	0.13	0.01	0.22		
VL – IgG	0.751	1.25	0.732	1.08		
12	0.01	0.20	0.02	0.20		
A-BETA	0.624	0.81	0.642	0.75	0.633	0.91
115	0.03	0.14	0.81	0.14	0.05	0.15
PATIENT	0.661	1.0	0.645	0.80	0.651	0.96
15 %	0.04	0.80	0.03	0.62	0.10	0.58
TAU	0.679	1.20	0.691	1.05	0.710	1.31
305	0.05	0.53	0.34	0.50	0.06	0.74
PATIENT	0.653	1.32	0.658	1.15	0.727	1.32
18 %	0.04	0.53	0.04	0.43	0.05	0.39
HEPARIN	0.723	1.61	0.750	1.55	0.837	4.20
2 %	0.07	0.57	0.05	0.40	0.05	2.25
LATE INTERMED. 3 %	0.694	1.19	0.680	1.03	0.685	0.96
	0.03	0.3	0.03	0.32	0.03	0.31
MID. INTERMED.	0.646	0.77	0.619	0.60	0.696	1.32
8 %	0.02	0.14	0.04	0.17	0.05	0.86
SALTS	0.677	1.22	0.664	0.99	0.686	1.05
5 %	0.04	0.82	0.06	0.69	0.03	0.32
PHF	0.662	1.37	0.671	1.25	0.743	1.53
13 %	0.01	0.11	0.02	0.18	0.02	0.18
α-SYNUCL	0.532	0.52	0.843	0.44	0.705	1.57
204	0.05	0.11	0.20	0.07	0.02	0.46
K< 0.5	0.479	0.39	0.473	0.30	0.700	1.62
56 %	0.06	0.38	0.06	0.10	0.05	0.62
0.5 <K< 1.0	0.701	0.72	0.765	0.83	1.018	1.31
34 %	0.03	0.08	0.06	0.10	0.05	0.49
K> 1.0	0.673	1.20	0.680	1.11	0.742	2.13
10 %	0.02	0.11	0.03	0.18	0.02	0.70
PATIENT	0.510	0.44	0.506	0.38	0.707	1.50
49 %	0.09	0.24	0.09	0.20	0.03	0.37

The available algorithms, which are oriented towards the simulation of structural changes, have been available for a long time and are currently being developed: TANGO [55,56], Aggrescan4D [57,58] take into account changing external conditions such as salt concentration, pH variation and temperature. However, the presence of these factors is taken into account at the atom-atom level. It is therefore a local impact. The positions of water molecules in the environment, as well as ions and other molecules, are determined by means of coordinates for these molecules. In the model presented herein, the external environment is treated as a continuum and expressed by means of an external force field (Eq. 6). The FOD-M model records the state structure of a molecule as the effect of the external force field on the organisation of hydrophobicity. An external force field affects the entire molecule, whereas an atom-atom interaction is strictly local and random.

Temperature mainly influences the internal force field, giving individual atoms the appropriate kinetic energy. It is not impossible that the polarity/hydrophobicity of the aquatic environment is affected by temperature. The structure and properties of water, especially in the context mentioned, are not recognised. The relationship between these two opposing characteristics is the subject of analysis presented in numerous publications without a clear conclusion so far.

5. Conclusions

A change in environment has a significant impact on amyloid transformation. Chains with identical sequences adopt an amyloid structure that is radically different from the native one. According to the model used, amyloid transformation taking place under altered conditions can be simulated in an *in silico* experiment when an external force field is introduced into the energy optimisation conditions in addition to the internal force field. The form of the external force field in the form of a continuum function is a suitably modified 3D Gaussian function with an appropriate K parameter value. The value of this parameter determines the degree of modification of the polar water environment directing the folding process towards obtaining a hydrophobic core with polar surface arrangement with a centrally located hydrophobic nucleus and a polar surface. Modification of this field involves mitigating this tendency and even favouring, in some cases, a distribution of hydrophobicity close to a form of uniform hydrophobicity/polarity distribution.

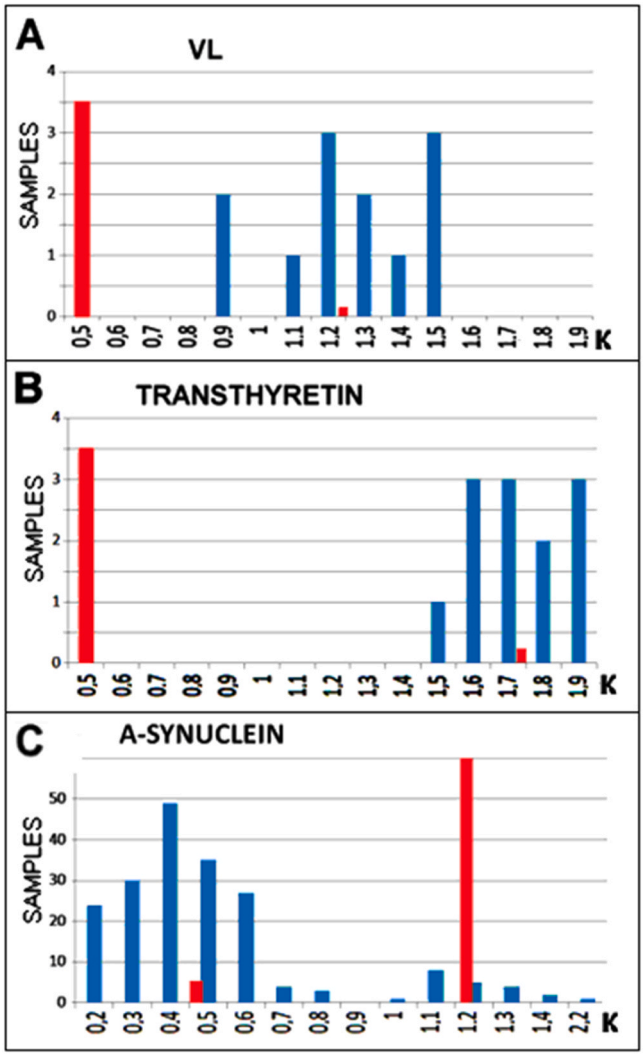

Fig. 5. Population analysis of structural characteristics expressed by K parameter of amyloid forms in:A – VL domain of IgG B – Transthyretin C – α-synuclein Red bars on left – status of native structure, red dot on x-axis – mean K value for all amyloid forms Vertical axis – number of examples of amyloids characterised by K values.

The dependence on the optimisation conditions in the amyloid transformation is included in the form of a funnel model designed to analyse the status of amyloid forms against native forms.

Application of this model reveals three distinct scenarios for the formation of amyloid forms. Transthyretin, VL domain of IgG shows a change from the hydrophobic burial form in which it functions under

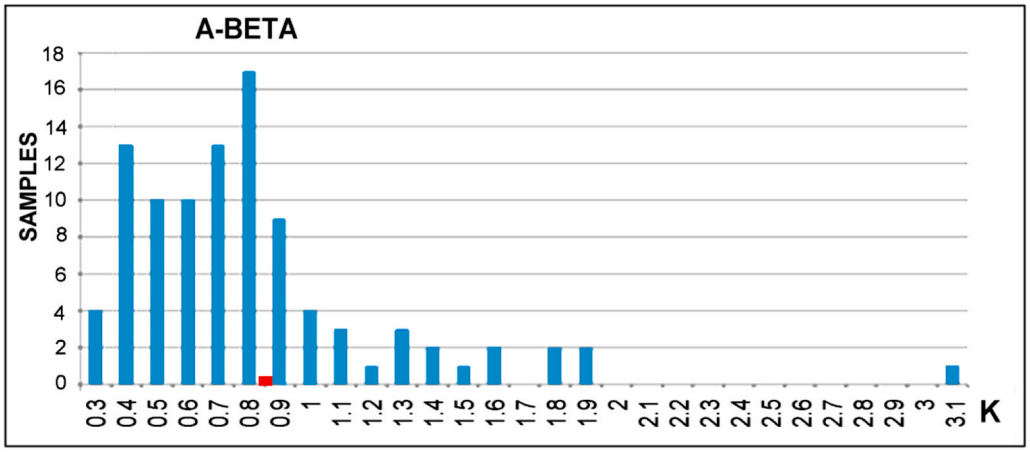

Fig. 6. Population analysis of structural characteristics expressed by K parameter (horizontal axis) of amyloid forms as observed in A-Beta amyloids Vertical axis – number of examples of amyloids characterised by K values.Red dot on x-axis – mean value of K for entire set of examples.

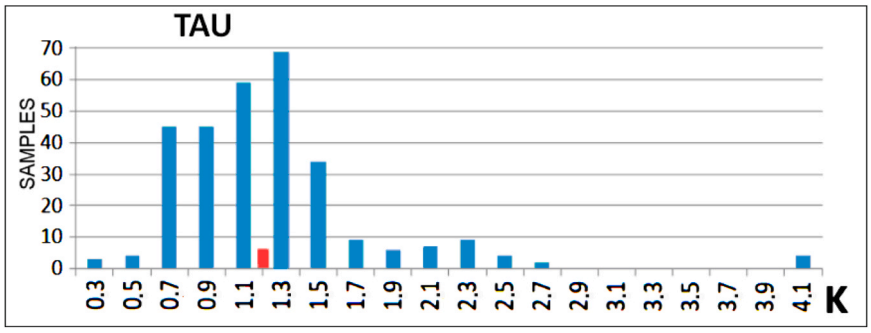

Fig. 7. Population analysis of structural characteristics expressed by K parameter of amyloid forms as observed in tau amyloids Vertical axis – number of examples of amyloids characterised by K values. Red dot on x-axis – mean value of K for entire set of examples. The position at K= 1.3 indicates the status of the 8PK4 fibril discussed earlier.

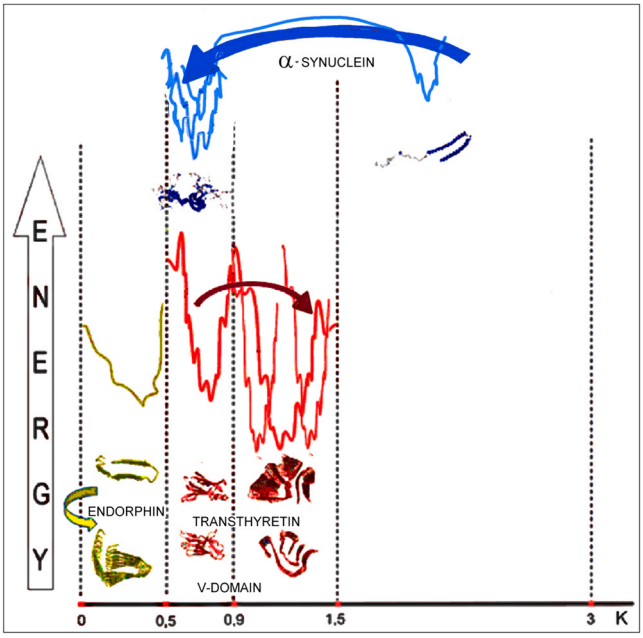

Fig. 8. Funnel model expressing environmental determinants (K values – horizontal axis) in relation to native structures and amyloid forms in pathological amyloids (α-synuclein, transthyretin, VL domain of IgG). The status of the functional amyloid – endorphin – is shown as unchanged in both forms: individual chain and fibril described by very low K values.

natural conditions, while the amyloid form is characterised by a significantly increased K parameter value. A different form is exhibited by α-synuclein, which in active conditions remains in complex with the axon terminals of presynaptic neurons, which is a factor that strongly imposes external force field conditions and thus is a source of high K values. Freed from interaction with the "permanent chaperone" that is the axon terminals of presynaptic neurons α-synuclein adapts to the conditions of polar water to form a hydrophobic collapse structure with a centrally located nucleus and a polar shell. A third scenario is provided by endorphin, which under natural conditions of biological activity has the structure of a typical amyloid fibril. The tau protein, whose model was analysed in this paper, also appears to belong to this group, indicating the first scenario. It is noted that the reference native structure of the tau protein is only of AF2 origin.

The dependence on the structuring (without changing the sequence) and thus the adoption of an optimal structure (low internal energy value) dependent on external conditions (external force field) can be demonstrated in the form of a funnel model. This has been demonstrated for biologically active proteins [51]. The innovation in the current analysis lies in the presentation of this model in quantitative form. The structural change (change in energy minimum) occurs depending on the value of the K parameter – the changed external force field conditions. Heterogeneous nucleation's role in amyloid formation interpreted on the basis of external conditions for the amyloid transformation process can be regarded as an effect of the active involvement of external conditions.

The biological meaning of the results is focused on the definition of the possible theoretical model allowing the process of protein

transformation to amyloid forms to be possible *in silico*. If the presented model appears adequate, the interpretation can be useful for practical use in research and therapy (external conditions for structural changes producing amyloids). The program for simulation *in silico* features in our group's plans.

Funding

Jagiellonian University Medical College: Grant # N41/DBS/001127.

Declaration of Competing Interest

All authors declare No Conflict of Interest.

Acknowledgements

The authors wish to thank to Anna Śmietańska and Zdzisław Wiśniowski for technical support. This research was carried out within the MSHE project "Support for the activity of Centers of Excellence established in Poland under Horizon 2020" on the basis of contract number MEiN/2023/DIR/3796. This project has received funding from the EU's Horizon 2020 research and innovation programme under grant agreement No. 857533. This publication is supported by the Sano ("Sano" – the name of project – in Latin means "Health") project carried out within the International Research Agendas programme of the FNP, co-financed by the EU under the European Regional Development Fund.

Data availability

The datasets used and/or analysed in the current study are available from the corresponding author upon reasonable request. All results can be recalculated using the programs described in Methods. The programs are in the open-access system.

References

[1] Dygut J, Kalinowska B, Banach M, Piwowar M, Konieczny L, Roterman I. Structural interface forms and their involvement in stabilization of multidomain proteins or protein complexes. Int J Mol Sci 2016;17(10):1741. https://doi.org/10.3390/ijms17101741.
[2] Willbold D, Strodel B, Schröder GF, Hoyer W, Heise H. Amyloid-type protein aggregation and prion-like properties of amyloids. Chem Rev 2021;121(13):8285–307. https://doi.org/10.1021/acs.chemrev.1c00196.
[3] Sawaya MR, Hughes MP, Rodriguez JA, Riek R, Eisenberg DS. The expanding amyloid family: structure, stability, function, and pathogenesis. Cell 2021;184(19):4857–73. https://doi.org/10.1016/j.cell.2021.08.013.
[4] ⟨https://people.mbi.ucla.edu/sawaya/amyloidatlas/⟩ amyloid atlas – accessed July 2024.
[5] Goldschmidt L, Teng PK, Riek R, Eisenberg D. Identifying the amylome, proteins capable of forming amyloid-like fibrils. Proc Natl Acad Sci USA 2010;107(8):3487–92. https://doi.org/10.1073/pnas.0915166107.
[6] Balbirnie M, Grothe R, Eisenberg DS. An amyloid-forming peptide from the yeast prion Sup35 reveals a dehydrated beta-sheet structure for amyloid. Proc Natl Acad Sci USA 2001;98(5):2375–80. https://doi.org/10.1073/pnas.041617698.
[7] Lövestam S, Li D, Wagstaff JL, Kotecha A, Kimanius D, McLaughlin SH, Murzin AG, Freund SMV, Goedert Michel, Scheres M. SHW. Disease-specific tau filaments assemble via polymorphic intermediates. Nature 2024;625(7993):119–25. https://doi.org/10.1038/s41586-023-06788-w.
[8] Lövestam S, Koh FA, van Knippenberg B, Kotecha A, Murzin AG, Goedert M, Scheres SHW. Assembly of recombinant tau into filaments identical to those of Alzheimer's disease and chronic traumatic encephalopathy. Elife 2022;11:e76494. https://doi.org/10.7554/eLife.76494.
[9] Fitzpatrick AWP, Falcon B, He S, Murzin AG, Murshudov G, Garringer HJ, Crowther RA, Ghetti B, Goedert M, Scheres SHW. Cryo-EM structures of tau filaments from Alzheimer's disease. Nature 2017;547(7662):185–90. https://doi.org/10.1038/nature23002.
[10] Falcon B, Zivanov J, Zhang W, Murzin AG, Garringer HJ, Vidal R, Crowther RA, Newell KL, Ghetti B, Goedert M, Scheres SHW. Novel tau filament fold in chronic traumatic encephalopathy encloses hydrophobic molecules. Nature 2019;568(7752):420–3. https://doi.org/10.1038/s41586-019-1026-5.
[11] Banach M, Prymula K, Jurkowski W, Konieczny L, Roterman I. Fuzzy oil drop model to interpret the structure of antifreeze proteins and their mutants. J Mol Model 2012;18(1):229–37. https://doi.org/10.1007/s00894-011-1033-4.
[12] Banach M, Stapor K, Konieczny L, Fabian P, Roterman I. Downhill, ultrafast and fast folding proteins revised. Int J Mol Sci 2020;21(20):7632. https://doi.org/10.3390/ijms21207632.
[13] Huang DB, Ainsworth CF, Stevens FJ, Schiffer M. Three quaternary structures for a single protein. Proc Natl Acad Sci USA 1996;93(14):7017–21. https://doi.org/10.1073/pnas.93.14.7017.
[14] Swuec P, Lavatelli F, Tasaki M, Paissoni C, Rognoni P, Maritan M, Brambilla F, Milani P, Mauri P, Camilloni C, Palladini G, Merlini G, Ricagno S, Bolognesi M. Cryo-EM structure of cardiac amyloid fibrils from an immunoglobulin light chain AL amyloidosis patient. Nat Commun 2019;10(1):1269. https://doi.org/10.1038/s41467-019-09133-w.
[15] Klabunde T, Petrassi HM, Oza VB, Raman P, Kelly JW, Sacchettini JC. Rational design of potent human transthyretin amyloid disease inhibitors. Nat Struct Biol 2000;7(4):312–21. https://doi.org/10.1038/74082.
[16] Schmidt M, Wiese S, Adak V, Engler J, Agarwal S, Fritz G, Westermark P, Zacharias M, Fändrich M. Cryo-EM structure of a transthyretin-derived amyloid fibril from a patient with hereditary ATTR amyloidosis. Nat Commun 2019;10(1):5008. https://doi.org/10.1038/s41467-019-13038-z.
[17] Ulmer TS, Bax A, Cole NB, Nussbaum RL. Structure and dynamics of micelle-bound human alpha-synuclein. J Biol Chem 2005;280(10):9595–603. https://doi.org/10.1074/jbc.M411805200.
[18] Tuttle MD, Comellas G, Nieuwkoop AJ, Covell DJ, Berthold DA, Kloepper KD, Courtney JM, Kim JK, Barclay AM, Kendall A, Wan W, Stubbs G, Schwieters CD, Lee VMY, George JM, Rienstra CM. Solid-state NMR structure of a pathogenic fibril of full-length human α-synuclein. Nat Struct Mol Biol 2016;23(5):409–15. https://doi.org/10.1038/nsmb.3194.
[19] Schweighauser M., Shi Y., Tarutani A., Kametani F., Murzin A.G., Ghetti B., Matsubara T., Tomita T., Ando T., Hasegawa K., Murayama S., Yoshida M., Hasegawa M., Scheres S.H.W., Goedert M. – PDB 6XYO.
[20] Fitzpatrick AWP, Falcon B, He S, Murzin AG, Murshudov G, Garringer HJ, Crowther RA, Ghetti B, Goedert M, Scheres SHW. Cryo-EM structures of tau filaments from Alzheimer's disease. Nature 2017;547(7662):185–90. https://doi.org/10.1038/nature23002.
[21] Seuring C, Verasdonck J, Gath J, Ghosh D, Nespovitaya N, Wälti MA, Maji SK, Cadalbert R, Güntert P, Meier BH, Riek R. The three-dimensional structure of human β-endorphin amyloid fibrils. Nat Struct Mol Biol 2020;27(12):1178–84. https://doi.org/10.1038/s41594-020-00515-z.
[22] Puri S, Gadda A, Polsinelli I, Barzago MM, Toto A, Sriramoju MK, Visentin C, Broggini L, Bonnet DMV, Russo R, Chaves-Sanjuan A, Merlini G, Nuvolone M, Palladini G, Gianni S, Hsu S-TD, Diomede L, Ricagno S. The critical role of the variable domain in driving proteotoxicity and aggregation in full-length light chains. J Mol Biol 2025;437(5):168958. https://doi.org/10.1016/j.jmb.2025.168958.
[23] Ueda M. Transthyretin: its function and amyloid formation. Neurochem Int 2022;155:105313. https://doi.org/10.1016/j.neuint.2022.105313.
[24] Twohig D, Nielsen HM. alpha-synuclein in the pathophysiology of Alzheimer's disease. Mol Neurodegener 2019;14(1):23. https://doi.org/10.1186/s13024-019-0320-x.
[25] Lei P, Ayton S, Finkelstein DI, Adlard PA, Masters CL, Bush AI. Tau protein: relevance to Parkinson's disease. Int J Biochem Cell Biol 2010;42(11):1775–8. https://doi.org/10.1016/j.biocel.2010.07.016.
[26] Jouanne M, Rault S, Voisin-Chiret AS. Tau protein aggregation in Alzheimer's disease: an attractive target for the development of novel therapeutic agents. Eur J Med Chem 2017;139:153–67. https://doi.org/10.1016/j.ejmech.2017.07.070.
[27] Amir S, Brown ZW, Amit Z. The role of endorphins in stress: evidence and speculations. Neurosci Biobehav Rev 1980;4(1):77–86. https://doi.org/10.1016/0149-7634(80)90027-5.
[28] Roterman I, Konieczny L. Protein is an intelligent Micelle. Entropy 2023;25(6):850. https://doi.org/10.3390/e25060850.
[29] Konieczny L, Brylinski M, Roterman I. Gauss-function-Based model of hydrophobicity density in proteins. Silico Biol 2006;6(1-2):15–22.
[30] Levitt MA. A simplified representation of protein conformations for rapid simulation of protein folding. J Mol Biol 1976;104:59–107. https://doi.org/10.1016/0022-2836(76)90004-8.
[31] Kalinowska B, Banach M, Konieczny L, Roterman I. Application of divergence entropy to characterize the structure of the hydrophobic core in DNA interacting proteins. Entropy 2015;17(3):1477–507. https://doi.org/10.3390/e17031477.
[32] Kullback S, Leibler RA. On information and sufficiency. Ann Math Stat 1951;22:79–86. https://doi.org/10.1214/aoms/1177729694.
[33] ⟨https://www.ks.uiuc.edu/Research/vmd/⟩.
[34] Humphrey W, Dalke A, Schulten K. VMD: visual molecular dynamics. 27-8 J Mol Graph 1996;14(1):33–8. https://doi.org/10.1016/0263-7855(96)00018-5.
[35] Frey L, Ghosh D, Qureshi BM, Rhyner D, Guerrero-Ferreira R, Pokharna A, Kwiatkowski W, Serdiuk T, Picotti P, Riek R, Greenwald J. On the pH-dependence of α-synuclein amyloid polymorphism and the role of secondary nucleation in seed-based amyloid propagation. Elife 2024;12:RP93562. https://doi.org/10.7554/eLife.93562.
[36] RotermanI, Stapor K, Dulak D, Fabian P, Konieczny L. Endorphin-functional amyloid with controlled fibril length. J Biotechnol Biomed 2025;8:10–20. https://doi.org/10.26502/jbb.2642-91280177.
[37] Eisenberg D, Jucker M. The amyloid state of proteins in human diseases. Cell 2012;148(6):1188–203. https://doi.org/10.1016/j.cell.2012.02.022.
[38] Chiti F, Dobson CM. Protein misfolding, functional amyloid, and human disease. Annu Rev Biochem 2006;75:333–66. https://doi.org/10.1146/annurev.biochem.75.101304.123901.

[39] Kayed R, Head E, Thompson JL, McIntire TM, Milton SC, Cotman CW, Glabe CG. Common structure of soluble amyloid oligomers implies common mechanism of pathogenesis. Science 2003;300(5618):486–9. https://doi.org/10.1126/science.1079469.
[40] Sternke-Hoffmann R, Sun X, Menzel A, Pinto MDS, Venclovaite U, Wördehoff M, Hoyer W, Zheng W, Luo J. Phase separation and aggregation of alpha-synuclein diverge at different salt conditions. Adv. Sci. 2024;11(34):e2308279. https://doi.org/10.1002/advs.202308279.
[41] Dułak D, Gadzała M, Banach M, Konieczny L, Roterman I. Alternative structures of alpha-Synuclein. Molecules 2020;25(3):600. https://doi.org/10.3390/molecules25030600.
[42] Roterman I, Dułak D, Gadzała M, Banach M, Konieczny L. Structural analysis of the Aβ(11-42) amyloid fibril based on hydrophobicity distribution. J Comput Aided Mol Des 2019;33(7):665–75. https://doi.org/10.1007/s10822-019-00209-9.
[43] Gadzała M., Dułak D., Banach M., Konieczny L., Roterman I., Stapor K., Fabian P. Folding with the active participation of water. In: From globular proteins to amyloids. Ed: Irena Roterman-Konieczna, Elsevier 2020, pp. 13-26. ⟨https://www.sciencedirect.com/book/9780081029817/from-globular-proteins-to-amyloids⟩.
[44] Zhang Y. I-TASSER server for protein 3D structure prediction. BMC Bioinforma 2008;9(1):40. https://doi.org/10.1186/1471-2105-9-40.
[45] Roy A, Kucukural A, Zhang Y. I-TASSER: a unified platform for automated protein structure and function prediction. Nat Protoc 2010;5(4):725–38. https://doi.org/10.1038/nprot.2010.5.
[46] Yang J, Yan R, Roy A, Xu D, Poisson J, Zhang Y. The I-TASSER suite: protein structure and function prediction. Nat Methods 2015;12(1):7–8. https://doi.org/10.1038/nmeth.3213.
[47] ⟨https://zhanglab.ccmb.med.umich.edu/I-TASSER⟩. Accessed 20 July 2018.
[48] ⟨http://robetta.org⟩. Accessed 20 July 2018.
[49] Kim DE, Chivian D, Baker D. Protein structure prediction and analysis using the Robetta server. Nucleic Acids Res 2004;32(Web Server):W526–31. https://doi.org/10.1093/nar/gkh468.
[50] Ferreon ACM, Deniz AA. Alpha-synuclein multistate folding thermodynamics: implications for protein misfolding and aggregation. Biochemistry 2007;46(15):4499–509. https://doi.org/10.1021/bi602461y.
[51] Roterman I, Slupina M, Konieczny L. Protein folding: Funnel model revised. Comput Struct Biotechnol J 2024;23:3827–38. https://doi.org/10.1016/j.csbj.2024.10.030.
[52] Franzmeier N, Roemer-Cassiano SN, Bernhardt AM, Dehsarvi A, Dewenter A, Steward A, Biel D, Frontzkowski L, Zhu Z, Gnörich J, Pescoller J, Wagner F, Hirsch F, de Bruin H, Ossenkoppele R, Palleis C, Strübing F, Schöll M, Levin J, Brendel M, Höglinger GU. Alpha synuclein co-pathology is associated with accelerated amyloid-driven tau accumulation in Alzheimer's disease. Mol Neurodegener 2025;20(1):31. https://doi.org/10.1186/s13024-025-00822-3.
[53] Hamidreza H.; Modjtaba R. A multi-objective gravitational search algorithm. In Computational Intelligence, Communication Systems and Networks *(CICSyN)*: 7–12.
[54] Goodarzi E, Ziaei M, Hosseinipour EZ. Introduction to optimization analysis in hydrosystem engineering. Berlin/Heidelberg: Springer; 2014. p. 111–48.
[55] Fernandez-Escamilla A-M, Rousseau F, Schymkowitz J, Serrano L. Prediction of sequence-dependent and mutational effects on the aggregation of peptides and proteins. Nat Biotechnol 2004;22(10):1302–6. https://doi.org/10.1038/nbt1012.
[56] ⟨https://software.embl-em.de/software/9⟩ - as accessed April 2025.
[57] Zalewski M, Iglesias V, Bárcenas O, Ventura S, Kmiecik S. Aggrescan4D: a comprehensive tool for pH-dependent analysis and engineering of protein aggregation propensity. Protein Sci 2024;33(10):e5180. https://doi.org/10.1002/pro.5180.
[58] Bárcenas O, Kuriata A, Zalewski M, Iglesias V, Pintado-Grima C, Firlik G, Burdukiewicz M, Kmiecik S, Ventura S. Aggrescan4D: structure-informed analysis of pH-dependent protein aggregation. Nucleic Acids Res 2024;52(W1):W170–5. https://doi.org/10.1093/nar/gkae382.